Measurement of the Ultrafast Spectral Diffusion of the Optical Transition of Nitrogen Vacancy Centers in Nano-Size Diamond Using Correlation Interferometry

Janik Wolters,[*] Nikola Sadzak, Andreas W. Schell, Tim Schröder, and Oliver Benson

Nano-Optics, Institute of Physics, Humboldt-Universität zu Berlin, Newtonstrasse 15, D-12489 Berlin, Germany

Spectral diffusion is the phenomenon of random jumps in the emission wavelength of narrow lines. This phenomenon is a major hurdle for applications of solid state quantum emitters like quantum dots, molecules, or diamond defect centers in an integrated quantum optical technology. Here, we provide further insight into the underlying processes of spectral diffusion of the zero-phonon line of single nitrogen vacancy centers in nano-size diamond by using a novel method based on photon correlation interferometry. The method works although the spectral diffusion rate is several orders of magnitude higher than the photon detection rate and thereby improves the time resolution of previous experiments with nano-size diamond by 6 orders of magnitude. We study the dependency of the spectral diffusion rate on the excitation power, temperature, and excitation wavelength under off-resonant excitation. Our results bring insight into the mechanism of spectral diffusion and suggest a strategy to increase the number of spectrally indistinguishable photons emitted by diamond nanocrystals.

In the last decade the negatively charged nitrogen vacancy (NV) center in diamond has emerged as a promising resource for future quantum technology [1–5]. NV centers, consisting of a nitrogen impurity atom with an adjacent vacancy, occur naturally in bulk diamond or diamond nanocrystals and are commonly used as single-photon sources, operating even at room temperature [6]. Diamond nanocrystals with a single NV are of particular interest, as they can be deterministically integrated into photonic and plasmonic hybrid devices and circuits [7–11]. The spectrum of the NV single-photon emission consists of a broad phonon sideband around 700 nm and a narrow zero-phonon line (ZPL) at about 638 nm. At cryogenic temperatures the ZPL of single NV centers in bulk type IIa diamond has been shown to be almost Fourier limited under off-resonant excitation, which allowed for the observation of two-photon interference [12,13], a crucial step toward applications in optical quantum information processing. However, for implanted NV centers located close to the surface, several GHz wide spectral diffusion can be observed under off-resonant illumination [14]. In nitrogen-rich type Ib nano-size diamond the energy levels fluctuate much stronger, leading to a broadened ZPL with a width of about 0.5 nm. It is widely assumed that line broadening of emitters in condensed phase is due to a fluctuating electrostatic environment [15,16]. In diamond nanocrystals it is caused by ionized impurities [17,18] and charge traps. The spectral shift caused by single charges can be estimated using a simple toy model [sketched in Fig. 1(a)]. Using data from Refs. [19,20] we found that the Stark shift of the excited states $\Delta \mathcal{E}_{x/y} = dE$ in an NV center induced by a single elementary charge in a distance of about 10 nm can be as large as several hundred GHz. The time after which the probability that the electrostatic environment remains

unchanged is reduced to $1/e$ can be defined as the spectral diffusion time τ_D. Within τ_D the system can be assumed to be free from spectral diffusion, and all photons emitted within τ_D should be nearly indistinguishable. Enhancing the number of indistinguishable subsequent photons is a key goal. In this Letter, we present measurements of τ_D in NV centers in nano-size diamond under off-resonant excitation with a time resolution exceeding previous experiments [21] with nano-size diamond by about 6 orders of magnitude. Our studies identify the excitation laser as the main source for enhanced spectral diffusion.

The most straightforward method to measure spectral diffusion in single emitters is to take a time series of spectra and directly visualize the spectral wandering [16,22,23]. However, this method is only suitable for low
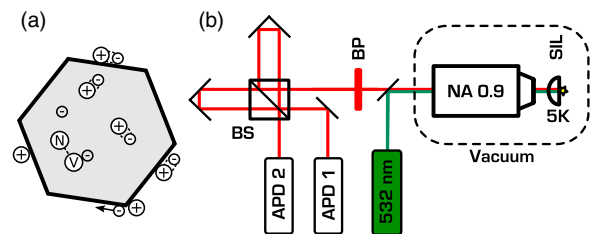

FIG. 1 (color online). (a) Toy model for spectral diffusion. Charge traps are ionized and lead to fluctuating electric fields at the NV center's location. (b) Sketch of the experimental setup. Milled type Ib nano-size diamond is deposited on a solid immersion lens (SIL) and placed in a continuos flow He cryostat. Single-photon fluorescence is excited with a 532 nm laser and collected through an objective lens with numerical aperture NA = 0.9. Using a spectral filter (BP) photons from the zero-phonon transition are filtered and sent through a folded Mach-Zehnder interferometer.

spectral diffusion rates. For many emitters, like NV centers in nano-size diamond the rate of detected photons emitted from the ZPL transition is on the order of a few kHZ, while spectral diffusion occurs much faster.

In the literature two methods that in principle enable spectral diffusion measurements on time scales as fast as the emitter's lifetime were suggested and demonstrated recently [24,25]. The idea is to convert the frequency fluctuations due to spectral diffusion into intensity fluctuations. However, in this approach, technical limitations such as the required complex setup with several moving parts reduced the time resolution in the first measurements to the order of 100 μs [24]. In a related approach Sallen *et al.* [22] reached the subnanosecond regime, but for the price of a spectrometer-limited spectral resolution and an inherently reduced detection efficiency. As pointed out in Ref. [26], this approach also requires the emission frequency to fluctuate around one fixed central wavelength, which is in general not the case for many quantum emitters.

Here, we use an advanced and simplified interferometric setup, combining the advantages of the previous approaches. The timing resolution is limited only by the single-photon counting instrumentation, which can be 100 ps or below. The spectral resolution can almost be as high as for conventional Fourier spectroscopy, while the central wavelength of the emission does not need to be fixed. Furthermore, the photon detection efficiency is at least doubled compared to the scheme presented in Ref. [22]. Therefore, our method is applicable even for moderate integration times.

We use a fixed Mach-Zehnder interferometer as a dispersing element, converting the spectral modulation of the ZPL into an intensity modulation that can be measured by correlating the photons from the two interferometer outputs. Figure 1(b) shows a sketch of the setup. From the measured photon statistics, the time scale of the spectral diffusion is derived. In the following we calculate the cross correlation between the outputs of the interferometer. We suppress the wavelength index λ of the photon number operator $\hat{n}_\lambda(t)$ for simplicity.

The time averaged photon detection rate in the left or right output port of the interferometer is $\langle \hat{I}(t)_{L\,(R)}\rangle_t$, with

$$\hat{I}(t)_{L\,(R)} = \eta_{L(R)}\hat{n}(t)m_{L\,(R)}(t), \qquad (1)$$

where $\eta_{L\,(R)}$ is the overall quantum efficiency in the left (right) exit of the interferometer, respectively. $m_{L(R)}(t)$ is the interferometer introduced modulation

$$m_{L\,(R)}(t) = 1 \pm c\sin[2\pi x/\lambda(t)], \qquad (2)$$

where c is the contrast of the interference fringes and x the path length difference of the interferometer arms. The plus and minus signs correspond to the left and right arm, respectively. The cross correlation between the two arms $g_{LR}^{(2)}(\tau) = (\langle :\hat{I}_L(t)\hat{I}_R(t+\tau):\rangle_t)/(\langle \hat{I}_L(t)\rangle_t \langle \hat{I}_R(t)\rangle_t)$ reads

$$g_{LR}^{(2)}(\tau) = g^{(2)}(\tau)\langle m_L(t)m_R(t+\tau)\rangle_t, \qquad (3)$$

where $g^{(2)}(\tau) = (\langle :\hat{n}(t)\hat{n}(t+\tau):\rangle_t)/(\langle \hat{n}(t)\rangle_t)$ is the second-order autocorrelation function of the bare emitter and $\langle :\dots :\rangle_t$ denotes normal ordering before time averaging.

We assume that spectral diffusion occurs in the form of jumps of the narrow emission line to random positions within a broad envelope [21] and that individual jumps lead to a significant change of the interferometer transmission. To calculate $\langle m_L(t)m_R(t+\tau)\rangle_t$ the characteristic function $X(t,\tau)$, which is one if no spectral jump occurred within the time interval $(t,t+\tau)$ and zero otherwise, is introduced and terms with and without spectral jump are separated in the average. By using that $\lambda(t) = \lambda(t+\tau)$ if no jump occurred and $\lambda(t+\tau) = \lambda(t') \neq \lambda(t)$ if a jump occurred, separating $X(t,\tau)$ and identifying the probability that the spectral position remains unchanged after the time τ as $p(\tau) = \langle X(t,\tau)\rangle_t$ we get

$$\langle m_L(t)m_R(t+\tau)\rangle_t = p(\tau)\langle m_L(t)m_R(t)\rangle_t$$
$$+ [1 - p(\tau)]\langle m_L(t)m_R(t')\rangle_{t,t'}. \qquad (4)$$

If the interferometer is adjusted in a way that several fringes are within the inhomogeneous width of the ZPL the sine terms average out and $\langle m_L(t)m_R(t')\rangle_{t,t'} = 1$, while $\langle m_L(t)m_R(t)\rangle_t = 1 - c^2/2$. Therefore

$$\langle m_L(t)m_R(t+\tau)\rangle_t = 1 - \left(\frac{c^2}{2}\right)p(\tau). \qquad (5)$$

Remarkably, here also path length fluctuations on time scales slower than the SD average out and interferometric stability is not required. Finally, the probability that the spectral position of the ZPL remains unchanged after some time τ is

$$p(\tau) = \frac{2}{c^2}\left(1 - \frac{g_{LR}^{(2)}(\tau)}{g^{(2)}(\tau)}\right). \qquad (6)$$

Thus, it is sufficient to measure the autocorrelation $g^{(2)}(\tau)$ of the bare emitter and the cross correlation between the two outputs L and R of the interferometer $g_{LR}^{(2)}(\tau)$ to gain knowledge of the spectral dynamics of the emitter. Nanocrystals milled from high-quality type Ib bulk diamond with a size of 30 nm to 100 nm were spin coated on a SIL made of zirconium dioxide [27]. The SIL is placed in a continuous flow He cryostat at about 5 K. Fluorescence is excited and collected in a confocal configuration [see Fig. 1(b)] through a commercial NA 0.9 objective lens (Mitutoyo) placed inside the isolation vacuum of the cryostat. The NV centers are excited by a green 532 nm laser with a power of several μW in front of the vacuum chamber. The single photons emitted by the NV are collected through the same objective lens and separated by a dichroic mirror from the excitation beam. An additional longpass filter blocks the excitation laser. In order to suppress the phonon sideband, a removable bandpass filter (width 7 nm) centered at 637 nm is used. The filtered photons are directed into a Mach-Zehnder interferometer

and detected by two avalanche photo diodes (APD) in the two outputs and counted with a time-correlated single-photon counting module (PicoQuant). The arm length difference of the interferometer was adjusted to obtain four fringes per nm at 639 nm, the ZPL wavelength (see Fig. 2). To check the alignment of the interferometer one of the APDs was replaced by a 500 mm spectrograph (Acton SpectraPro 500i) with a cooled CCD detector and spectra were recorded (see Fig. 2).

In order to derive the probability $p(\tau)$ that the spectral position remains unchanged after the time τ according to Eq. (6), first the bare second-order autocorrelation of the NV emission has to be measured. In order to do this, the whole fluorescence from the NV including phonon side-bands is sent into the interferometer. In this case the autocorrelation function $g^{(2)}(\tau)$ measured by the two APDs is unaffected by the interferometer as proven by an independent measurement. The setup acts as a usual Hanbury Brown and Twiss setup. Next, the 637 nm band-pass filter is added in front of the interferometer and the cross correlation $g_{LR}^{(2)}(\tau)$ between the interferometer arms is measured with a typical integration time of 30 min. In this case the interferometer converts the spectral jumps of the narrow ZPL emission into intensity fluctuations. Care was taken not to change the laser power or adjustment within the total measurement time. The measured $g^{(2)}$- and $g_{LR}^{(2)}$-functions of NV center 1 taken at an excitation laser power of 14.1 μW are shown in Fig. 3(a). In order to derive the spectral diffusion probability $p(\tau)$ the data is evaluated according to Eq. (6), resulting in the data shown in Fig. 3(b). Measurements taken with different interferometer adjustments revolving around spectral jump widths from 260 to 20 GHz showed that the assumption of a narrow line jumping in a broad envelope is well justified
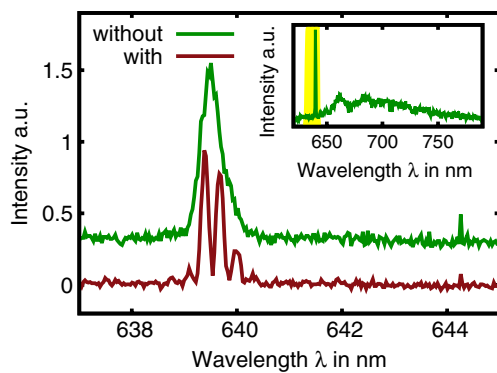
(see Supplemental Material [28]). The integration time of 30 min was sufficiently long to resolve the spectral diffusion, but if higher timing resolution is needed the integration time must be increased. The decrease of the probability $p(\tau)$ fits well to a single exponential decay. This supports the assumption that spectral diffusion is indeed caused by uncorrelated charge fluctuations. The spectral diffusion time τ_D obtained from the fit is 4.6 ± 0.6 μs corresponding to a spectral diffusion rate $\gamma_D = 1/\tau_D$ of about 220 kHz, while detection rate at the APDs of photons from the ZPL transition is only 2.3 kHz.

The achieved contrast c derived from the fit is 35%, which is lower than the measured interferometer contrast of 90% due to fluorescence background and the two non-degenerate NV dipole transitions [20].

To get further insight into the origin of the spectral diffusion, we measured the dependency of the spectral diffusion rate γ_D on the excitation power on NV center 1. Therefore, the above described measurement was repeated for several laser powers between 3 and 23 μW, well below the saturation power. The resulting data [Fig. 4(a)] show a clear linear dependency, a feature that was also observed on NV center 3 where we repeated the measurement (see Supplemental Material [28]). Thereby we can rule out two photon processes like the photoinduced charge conversion [29] to be the origin of spectral diffusion. Remarkably for zero excitation power, the spectral diffusion rate reaches zero within the precision of the fit, although the intersection with the axis is a free fit parameter. From this we make two conclusions: First, the excitation with the green laser is the main cause of spectral diffusion. This is consistent with our simple charge trap model. The laser ionizes impurities, providing floating charges that can be trapped in other charge traps.

FIG. 2 (color online).   Spectra of the ZPL from a typical nano-size diamond at a temperature of 5 K with a removable bandpass filter centered at the ZPL (637 nm). The green curve (upshifted by 0.3 for clarity) is the NV center's fluorescence measured without the interferometer. The lower red curve is recorded after the interferometer. The inset shows the full NV spectrum with the yellow shaded area indicating the transmission of the band-pass filter.
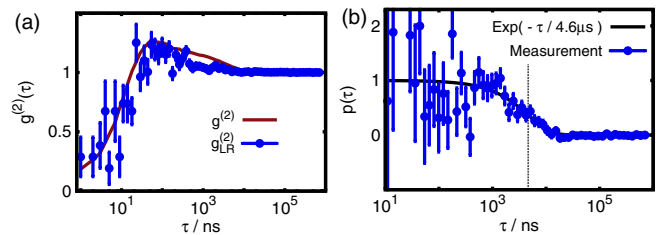

FIG. 3 (color online).   (a) Measured second-order autocorrelation function $g^{(2)}(\tau)$ (red line) and cross correlation $g_{LR}^{(2)}(\tau)$ (blue dots) of NV center 1 at an excitation laser power of 14.1 μW. The bin size is increased for longer delays τ, to decrease the error. The error of $g^{(2)}(\tau)$ is in the order of the linewidth. The dip at zero time delay shows the single-photon character of the emission. (b) The probability $p(\tau)$ that the ZPL remains constant on the order of 100 GHz within the time interval τ calculated from the data shown in (a) according to Eq. (6). The bin size is increased for longer delays τ, to decrease the error. The black line is an exponential fit to the data showing a spectral diffusion time τ_D of (4.6 ± 0.6) μs, while the dashed black line indicates the spectral diffusion time τ_D ($1/e$ time).
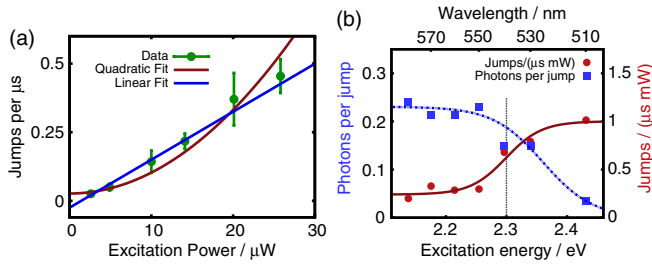
FIG. 4 (color online). (a) Dependency of the spectral diffusion rate on the excitation power, measured on NV center 1. The straight line is a linear fit to the data with the jump rate at zero excitation power being a free fit parameter. The bend curve is a quadratic fit to the data. (b) The number of collected photons from the ZPL transition per spectral jump as a function of the excitation photon energy, as measured on NV center 2. The square data points were measured at equal photon count rates and varying excitation powers (left axis). Point size corresponds to the error bar. The dashed curve is a guide to the eyes. The circles show the spectral jump rate normalized to the excitation power, calculated from the same data set (right axis). It is clearly visible that the spectral diffusion rate increases dramatically above the threshold of about 2.3 eV.

Second, the number of collected photons in the ZPL collected per spectral jump is constant for excitation far below saturation, i.e., independent of the excitation power. This number directly evaluates the quality of the single-photon emission in terms of the possible number of subsequent indistinguishable photons available. This is a key figure of merit for future quantum optics experiments with NV centers. Obviously, in the linear regime of excitation power (far below saturation) the quality of single-photon emission cannot be improved by reducing the excitation laser power, as it is often done in experiments with self-assembled quantum dots [30].

In order to derive a strategy to increase the number of collected photons per spectral jump we investigated its dependency on the temperature and excitation energy. Within the temperature range of 5–20 K we did not observe any change in the spectral diffusion rate on NV center 1. This is again consistent with the laser being the main cause of spectral diffusion by ionization of charge traps since their ionization energy exceeds $k_b T$ at this temperature range. In order to measure the influence of the excitation energy, we replaced the 532 nm cw laser with a pulsed super continuum source (NKT Photonics) with exchangeable 10 nm broad bandpass filters. While keeping the count rate in the ZPL constant at (1.4 ± 0.2) kcts/s (well below saturation) we measured the spectral diffusion rate of NV center 2 for several excitation wavelengths from 510 to 580 nm, corresponding to photon energies between 2.1 and 2.4 eV. We plotted the number of collected photons in the ZPL per spectral jump and the spectral jump rate normalized to the excitation power. The measurement in Fig. 4(b) clearly indicates that the number of collected photons per spectral jump decreases and spectral diffusion rate

increases with increasing excitation energy. Remarkably, there is a pronounced threshold of about 2.3 eV. This gives evidence for the existence of deep charge traps with an ionization energy close to 2.3 eV. The remaining spectral diffusion for energies below threshold might be attributed to substitutional nitrogen atoms in the diamond nanocrystals forming donor levels that are ionized at 1.7 eV [17,18]. More extensive studies to identify the trap states as well as to generally modify these states in order to reduce spectral diffusion and studies of higher quality diamond with natural or implanted defects will be a subject of future work. Furthermore, using two color excitation, the studies can be extended to energies below the ZPL transition to investigate the influence of the nitrogen donors at 1.7 eV.

In conclusion, we present an interferometric method to measure the spectral diffusion of the ZPL of single nitrogen vacancy centers in nano-size diamond. Our method works even if the spectral diffusion rate is orders of magnitudes higher than the photon detection rate and it is applicable for moderate integration times. Our systematic studies show that in milled type Ib nano-size diamond the jump rate is 1–2 orders of magnitude higher than the photon collection rate. Furthermore, the jump rate per photon is independent of the excitation power and NV temperature but depends strongly on the excitation wavelength. Our results support the assumption that the main source of spectral diffusion stems from charge traps. A promising strategy to maximize the number of subsequent single photons from a nano-size diamond is to use relatively high excitation powers, but clearly below the saturation level, and to choose a proper low excitation wavelength. Actively enhancing the optical transition strength [7,11] or collection rate is also required, possibly to enable active line stabilization schemes, as reported for NV centers in bulk diamond [20]. Finally, surface treatment accompanied by ultrafast spectral diffusion studies should be extended to learn more about the dynamics of trap states on the diamond surface.

*janik.wolters@physik.hu-berlin.de
[1] I. Aharonovich, A. D. Greentree, and S. Prawer, Nat. Photonics **5**, 397 (2011).
[2] J. L. O'Brien, A. Furusawa, and J. Vuckovic, Nat. Photonics **3**, 687 (2009).
[3] R. Hanson and D. D. Awschalom, Nature (London) **453**, 1043 (2008).
[4] T. D. Ladd, F. Jelezko, R. Laflamme, Y. Nakamura, C. Monroe, and J. L. O'Brien, Nature (London) **464**, 45 (2010).

[5] F. Jelezko and J. Wrachtrup, Phys. Status Solidi A **203**, 3207 (2006).

[6] J. Wrachtrup and F. Jelezko, J. Phys. Condens. Matter **18**, S807 (2006).

[7] O. Benson, Nature (London) **480**, 193 (2011).

[8] D. Englund, B. Shields, K. Rivoire, F. Hatami, J. Vuckovic, H. Park, and M. D. Lukin, Nano Lett. **10**, 3922 (2010).

[9] T. van der Sar, J. Hagemeier, W. Pfaff, E. C. Heeres, S. M. Thon, H. Kim, P. M. Petroff, T. H. Oosterkamp, D. Bouwmeester, and R. Hanson, Appl. Phys. Lett. **98**, 193103 (2011).

[10] J. Wolters, A. W. Schell, G. Kewes, N. Nusse, M. Schoengen, H. Doscher, T. Hannappel, B. Lochel, M. Barth, and O. Benson, Appl. Phys. Lett. **97**, 141108 (2010).

[11] J. Wolters et al., Phys. Status Solidi B **249**, 918 (2012).

[12] H. Bernien, L. Childress, L. Robledo, M. Markham, D. Twitchen, and R. Hanson, Phys. Rev. Lett. **108**, 043604 (2012).

[13] A. Sipahigil, M. Goldman, E. Togan, Y. Chu, M. Markham, D. Twitchen, A. Zibrov, A. Kubanek, and M. Lukin, Phys. Rev. Lett. **108**, 143601 (2012).

[14] K.-M. C. Fu, C. Santori, P. E. Barclay, and R. G. Beausoleil, Appl. Phys. Lett. **96**, 121907 (2010).

[15] A. Majumdar, E. D. Kim, and J. Vuckovic, Phys. Rev. B **84**, 195304 (2011).

[16] J. Wrachtrup et al., in Single Molecule Detection in Solution, edited by C. Zander, J. Enderlein, and R. A. Keller (Wiley-VCH, Berlin, 2002).

[17] R. G. Farrer, Solid State Commun. **7**, 685 (1969).

[18] J. Rosa, M. Vanecek, M. Nesladek, and L. M. Stals, Diam. Relat. Mater. **8**, 721 (1999).

[19] Ph. Tamarat et al., Phys. Rev. Lett. **97**, 083002 (2006).

[20] V. M. Acosta et al., Phys. Rev. Lett. **108**, 206401 (2012).

[21] Y. Shen, T. M. Sweeney, and H. Wang, Phys. Rev. B **77**, 033201 (2008).

[22] G. Sallen, A. Tribu, T. Aichele, R. André, L. Besombes, C. Bougerol, M. Richard, S. Tatarenko, K. Kheng, and J.-Ph. Poizat, Nat. Photonics **4**, 696 (2010).

[23] U. W. Pohl et al., in Semiconductor Nanostructures, edited by D. Bimberg (Springer, Berlin, 2008).

[24] L. Coolen, X. Brokmann, P. Spinicelli, and J. P. Hermier, Phys. Rev. Lett. **100**, 027403 (2008).

[25] X. Brokmann, M. Bawendi, L. Coolen, and J.-P. Hermier, Opt. Express **14**, 6333 (2006).

[26] M. Orrit, Nat. Photonics **4**, 667 (2010).

[27] T. Schröder, F. Gädeke, M. J. Banholzer, and O. Benson, New J. Phys. **13**, 055017 (2011).

[28] See Supplemental Material at http://link.aps.org/supplemental/10.1103/PhysRevLett.110.027401 for additional measurements on NV center 3 and NV center 4.

[29] G. Waldherr, J. Beck, M. Steiner, P. Neumann, A. Gali, Th. Frauenheim, F. Jelezko, and J. Wrachtrup, Phys. Rev. Lett. **106**, 157601 (2011).

[30] H. D. Robinson and B. B. Goldberg, Phys. Rev. B **61**, R5086 (2000).